J. Med. Biol. Eng. (2016) 36:121–131
DOI 10.1007/s40846-016-0112-5

ORIGINAL ARTICLE

Muscle Strength Assessment System Using sEMG-Based Force Prediction Method for Wrist Joint

Songyuan Zhang[1] · Shuxiang Guo[2,3] · Baofeng Gao[2] · Qiang Huang[2] · Muye Pang[1] · Hideyuki Hirata[3] · Hidenori Ishihara[3]

Received: 20 April 2015 / Accepted: 30 September 2015 / Published online: 29 January 2016

Abstract Tele-assessment systems are crucial for home-based rehabilitation, as they allow therapists to assess the status of patients and adjust the parameters of various home-based training devices. Traditional force/torque sensors are commonly used in tele-assessment systems to detect muscle strength because such sensors are convenient. However, muscle activity can be measured using surface electromyography (sEMG), which records the activation level of skeleton muscles and is a more accurate method for determining the amount of force exerted. Thus, in this paper, a method for predicting muscle strength using only sEMG signals is proposed. The sEMG signals measure the isometric downward touch motions and are recorded from four muscles of the forearm. The prediction function is derived from a musculoskeletal model. The parameters involved are calibrated using the Bayesian linear regression algorithm. To avoid the complex modeling of the entire movement, a neural network classifier is trained to recognize the force-exerting motion. Experimental results show that the mean root-mean-square error of the proposed method is below 2.5 N. In addition, the effects of the high-pass cutoff frequency and the co-activation of flexors and extensors for EMG force prediction are discussed in this paper. The performance of the proposed method is validated further in real-time by a remote predicted-force evaluation experiment. A haptic device (Phantom Premium) is used to represent the predicted force at the therapist's remote site. Experimental results show that the proposed method can provide acceptable prediction results for tele-assessment systems.

Keywords Tele-assessment system · Muscle strength prediction · Surface electromyography · Classification · Bayesian linear regression · Co-activation · Haptic device

1 Introduction

Approximately 795,000 new or recurrent strokes are reported annually in the United States [1]. Compared with traditional physical therapy, which is labor-intensive and requires one-to-one therapist-patient interaction, therapeutic robots have been investigated by many researchers to make the process more practical and to ease the burden on therapists [2]. Although these devices can relieve the burden of physical therapy, most of them are bulky and cannot be moved. Thus, patients still have to travel to rehabilitation centers, which is an inconvenience that may interface with some patients' continuing rehabilitation. Therefore, tele-rehabilitation systems, which contain suitable home-based rehabilitation devices as well as tele-assessments, would be a significant step forward.

A previous study developed a portable exoskeleton device [3, 4]. The device serves as part of a patient's home-based rehabilitation. Because the pre-set training parameters should be determined for each patient by an experienced therapist, a tele-assessment system is required. Park

✉ Songyuan Zhang
s13d505@stmail.eng.kagawa-u.ac.jp

[1] Graduate School of Engineering, Kagawa University, Takamatsu, Kagawa 761-0396, Japan

[2] Institute of Advanced Biomedical Engineering System, School of Life Science and Technology, Key Laboratory of Convergence Medical Engineering System and Healthcare Technology, The Ministry of Industry and Information Technology, Beijing Institute of Technology, Haidian District, Beijing 100081, China

[3] Department of Intelligent Mechanical Systems Engineering, Kagawa University, Takamatsu, Kagawa 761-0396, Japan

et al. [5] developed a tele-assessment system for elbow joint spasticity in which a torque sensor is used to measure force/torque. However, comparatively, surface electromyography (sEMG), which records the activation level of skeleton muscles, is a more accurate method for obtaining the amount of force exerted. Thus, this study proposes a tele-assessment system that uses sEMG to predict the muscle force on the wrist joint.

In recent decades, the relationship between muscle force and sEMG signals has been extensively investigated [6, 7]. Savelberg and Herzog [8] used an artificial neural network (ANN) with a backpropagation algorithm to predict dynamic tendon forces from EMG signals. However, these authors applied a generalization of ANN to the representation of complex relationships between dynamic forces and EMG signals without any explicit function description. Conversely, Cavallaro et al. [9, 10] developed a myoprocessor based on Hill phenomenological muscular models, which implements a genetic algorithm to tune the parameters involved in muscular models and is a relatively explicit method for predicting the joint torques of upper limbs.

However, to study such relationships, both explicit and implicit methods require careful processing of sEMG signals and elaborate parameter calibration. According to one study [6], the validity of muscle force estimation using sEMG comprises several criteria, such as accurate estimation of muscle activation, nature of the EMG–force relationship, differences in temporal characteristics between EMG and force signals, normalization of the EMG amplitude, and effects of muscle contraction dynamics. To estimate muscle activation, Manal and Buchanan [11] proposed a one-parameter model for obtaining muscle activation from neural activation. The optimal parameter was determined iteratively using the Newton–Raphson method. A non-linear normalization method proposed by Potvin et al. [12] has also been applied [13–18].

Here, a muscle force prediction method for isometric downward touch motion that uses only sEMG signals is proposed. The predicated force is used to assess the muscle strength of patients. Unlike clinical studies of individual muscles (such as those mentioned above), the proposed method tries to predict contact force as an output of the function of muscle groups. The sEMG signals recorded from four muscles of the forearm are used for force prediction. The prediction function was derived from a dynamic equation based on an upper-limb musculoskeletal model, with muscle activation levels as the input. The parameters were calibrated using the Bayesian linear regression (BLR) algorithm. Because the total motion is dynamic, it is necessary to identify the force-exerting motion from other motions; in order to do so, and to avoid complex modeling of the entire movement, an ANN was applied to classify the force-exerting motion. Additionally, a remote force estimation experiment was designed to validate real-time performance. The effect of high-pass cutoff filtering and the co-activation of flexors and extensors for force prediction (root-mean-square (RMS) error and linear correlation coefficient (CC)) are also considered in order to improve the results.

2 Materials and Methods

2.1 Experimental Apparatus and Protocol

Seven male subjects without neuromuscular deficit (age: 25.67 ± 2.66 years, height: 1.71 ± 0.05 m, weight: 66.50 ± 9.04 kg) participated in the experiment. The experimental setup is shown in Fig. 1a. Prior to data

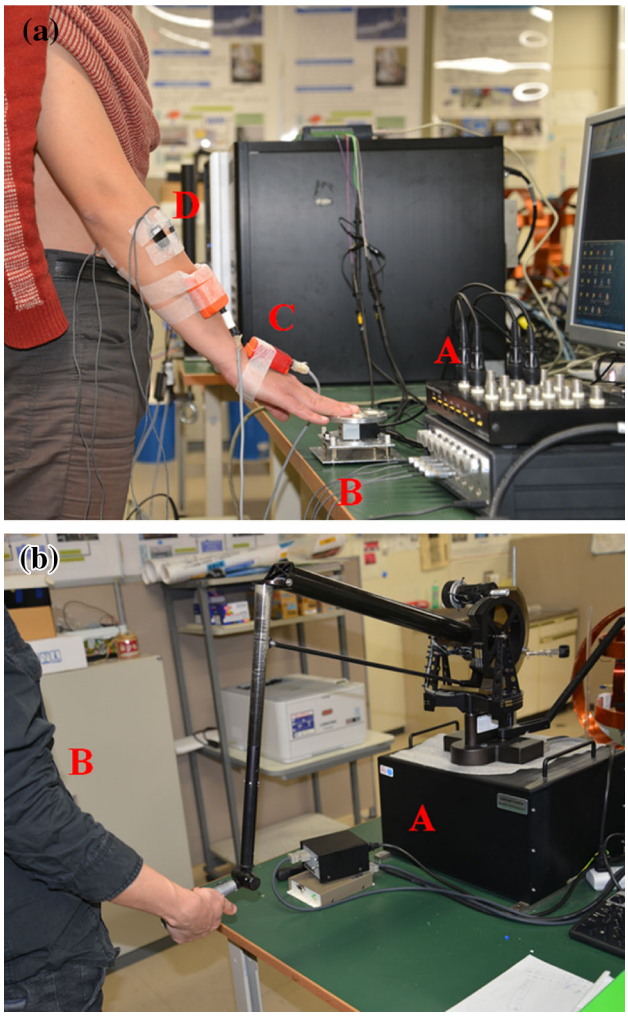

Fig. 1 **a** Downward touch motion (*A* signal acquisition device and filter box; *B* force sensor; *C* two MTx sensors; *D* electrodes mounted on correlative muscles). **b** Surrogate therapist operating haptic device (Phantom Premium) (*A* haptic device; *B* surrogate therapist)

collection, the subjects were shaved and wiped down with alcohol. Dry rectangular electrodes (Ag/AgCl, size: 26 × 14 mm, Oisaka Development Ltd., Japan), with a skin contact surface of 20 mm^2 and an inter-electrode distance of 15 mm, were placed parallel to the subjects' muscle fibers, according to SENIAM references [19]. Electrode placements were confirmed according to a method described in a previous study [20]. The recorded sEMG signals were pre-processed by a commercial filter box (10–500 Hz band pass, 60 Hz band rejection, amplified 1000×, Personal EMG, Oisaka Development Ltd., Japan) with differential amplification (gain: 1000) and common-mode rejection (104 dB) at a sampling frequency of 3000 Hz. They were then sampled at 1000 Hz by a 16-bit analog-to-digital (A/D) acquisition device (USB4716, 16-channel input, Advantech Co., Ltd., Taiwan).

When using EMG signals to predict muscle force, a movement-restricting apparatus is often used to constrain the joint angle of the upper limb being measured (e.g., a one-degree-of-freedom exoskeleton testbed [21]). Because the joint angle involves factors that affect the EMG–force relationship [21], this restriction of motion is necessary for the purposes of clinical study. In our study, MTx sensors (Xsens Technologies B.V., Enschede, The Netherlands) were attached to the subject's hand and forearm to record joint angles. A force sensor (ThinNANO, BL AUTOTEC, LTD., Japan) was mounted on a platform to record the subjects' downward touch force. A haptic device (Phantom Premium, Geomagic, USA) can be used to represent the predicted contact force to therapists at a remote location. Phantom Premium (shown in Fig. 1b) is a commercial haptic product with which haptic force can be exerted by the patient and remotely sensed by the operator via a handle.

During the downward touch motion, each subject was asked to touch the center of the force sensor with his index, middle, and ring fingers while keeping the entire palm flat. The hand faced downward while the forearm flexed approximately 30° and the wrist flexed approximately 45° (as shown in Fig. 1a). First, each subject found a comfortable position for performing the downward touch motion, and the joint angles were recorded for reference. Then, maximum voluntary contraction (MVC) tests were performed to record sEMG data for four forearm muscles. As part of the MVC tests, the subject was asked to press the force sensor (wrist flex) as hard as possible (a deviation in joint angle within 3° of its reference measurements indicated high joint stiffness) and to maintain that maximum level of force for 5 s. The sEMG data from this motion were recorded to obtain the MVC values for the flexor carpi radialis (FCR) and the flexor carpi ulnaris (FCU). The subject was then asked to perform the same gesture with the dorsal aspect of his hand against the underside of the platform while extending the wrist as much as possible and maintaining the same maximum level of force for 5 s. The sEMG data recorded for this motion were used to obtain the MVC values for the extensor carpi radialis longus (ECRL) and the extensor carpi ulnaris (ECU). Each trial was repeated three times with a 1-min rest in between; the highest value for each was treated as the MVC value.

After the MVC tests, subjects were asked to perform a downward touch experiment. The downward touch movement was divided into five steps: (1) an initial gesture with the upper limb in a relaxed position; (2) a reaching motion to touch the force sensor (lasting about 2 s); (3) a force-exerting motion (lasting about 5 s); (4) a return to the initial gesture (lasting about 2 s); and (5) the initial gesture. The experiment was divided into two groups, namely the offline and online groups. In the offline group, subjects performed the downward touch motion following a reference gesture. The maximum force amplitude ranged from 5 to 25 N, in increments of 5 N (i.e., total of 5 trials), and each trial was repeated five times with a rest time of 30 s in between. Then, the data were processed and ANNs were trained for each subject individually. In the online group, subjects were asked to perform the downward touch motion in a relatively free way (deviation of the joint angle from its reference was within 10°); the contact force was predicted in real-time, and there were five trials, just as with the offline group.

During the online evaluation, one surrogate therapist was asked to hold the handle of the haptic device in order to feel the contact force in a remote location. Because the maximum force provided by the haptic device is 22 N, the evaluation was graded into three levels: 0–5 N (low level), 5–10 N (medium level), and 10–15 N (high level). Prior to the experiment, a simulation test allowed the surrogate therapist to be familiarized with how each of the three levels would feel.

2.2 Data Processing and Analysis

The sEMG signal acquired from an A/D board was processed with a digital high-pass first-order Butterworth filter with cutoff frequencies of 20, 200, and 400 Hz, respectively, to compare the effects of high-pass cutoff frequency on downward touch force estimation. Post-processed sEMG signals were then full-wave rectified and low-pass filtered by a first-order Butterworth filter with a cutoff frequency of 2 Hz to acquire the envelope. Afterward, normalization was performed on the four channels of sEMG data by dividing the corresponding MVC values. The above process, following a previous study [11], was applied to transform raw sEMG signals to values called $e(t)$. A discretized second-order recursive filter with the

discrete form of Eq. (1) was implemented to obtain $u(t)$ from $e(t)$ [22]. In Eq. (1), d is the electromechanical delay and α, $\beta 1$, and $\beta 2$ are the coefficients that define the second-order dynamics. A detailed description of these parameters can be found elsewhere [23].

$$u(t) = \alpha e(t-d) - \beta_1 u(t-1) - \beta_2 u(t-2) \quad (1)$$

Non-linear processing was performed on $u(t)$ to obtain muscle activation $a(t)$:

$$a(t) = 100\frac{\exp(-u(t)\cdot c) - 1}{\exp(-100\cdot c) - 1} \quad (2)$$

where constant c was set at 0.02 for this study.

The raw signals from the force sensor, MTx sensors, and sEMG electrodes were sampled simultaneously and saved for further processing. Data from the force sensor were low-passed by a digital first-order Butterworth filter with a cutoff frequency of 2 Hz. The data recorded from the MTx sensors needed no further filtering since an embedded algorithm was used. Repeated measurements of one-way analysis of variance (ANOVA) were used with the high-pass cutoff frequency as a fixed factor and RMS errors and CCs between predicted results and measured ones as dependent variables. Furthermore, in order to determine the effect of flexor and extensor co-activation on prediction, another analysis was performed with and without using extensors as a fixed factor for prediction. The significance level was set at 0.05.

2.3 Schematic of Proposed Contact Force Prediction Method

A schematic of the proposed method is depicted in Fig. 2, including the offline calibration and online prediction. An ANN classifier was applied to classify the force-exerting motion and the BLR algorithm was adopted to calibrate the parameters involved in the prediction function. The input was the muscle activation levels of the four muscles and the output was the predicted contact force. The inputs were first recognized by the ANN classifier in order to separate the force-exerting motion from other motions. When the force-exerting motion was recognized, the muscle activation levels were used sequentially to predict the contact force. Details for each block in the schematic are provided in the following subsections.

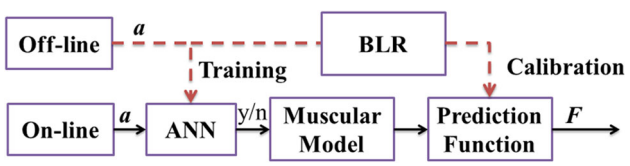

Fig. 2 Schematic of proposed downward touch force prediction method. a represents muscle activation level. ANN is classifier used to recognize force-exerting motion. BLR algorithm was adopted to calibrate parameters in prediction function

2.4 Motion Recognition

During muscle strength assessment, only the muscle activation for the exerting force is needed. However, the entire movement includes the relaxed phase, reaching phase, force-exerting phase, and returning phase. Although some researchers have developed explicit models to study the movement of upper limbs [24], the topic itself is challenging and additional sensors are needed; comparatively, the pattern recognition method using only sEMG signals [25–29] is more suitable for our case. The identified muscle activation for the exerting force was used for further force prediction.

In this paper, an ANN classifier was applied to identify the various motions. The muscle activation levels for each of the four muscles were the classifier's input; the binary representations of each of the four motions (relaxed, reaching, force-exerting, and returning) were the output. The training data were well labeled, according to the joint angles and force values. One set of the training data is shown in Fig. 3. The relaxed motion was labeled when there were no changes in joint angles or muscle activation levels. The reaching and returning motions were labeled when there were changes in joint angles but no change in force value. The force-exerting motion was labeled when the force value changed.

The ANN contained one hidden layer with eight neurons. The hyperbolic tangent sigmoid transfer function and scaled conjugate gradient backpropagation training algorithm were adopted for the hidden layer combination and learning process, respectively. The training process was conducted using MATLAB neural network recognition tools (Version 7.10.0.499, MathWorks, Inc., USA) and the online recognition was calculated by a modified C++ program, in which the parameters involved were obtained from the ANN training results from MATLAB.

In some cases, we found that the ANN classifier could not recognize a motion immediately; this is a problem in force prediction. Because the classifier cannot be guaranteed to recognize the force-exerting motion as soon as the subject exerts a force on an object, when the force-exerting motion is finally recognized, the predicted result will be discontinuous from the previous one (i.e., a zero value). Thus, the end result is also discontinuous. Thus, when the predicted force is transmitted to the therapist's location, a suddenly increased or decreased force will appear. In order to address this problem, we propose a proportional smoothing algorithm:

$$F_i' = F_i \mp (\Delta - \Delta \cdot i/t) \quad i = 1, 2, 3, \ldots, t \quad (3)$$

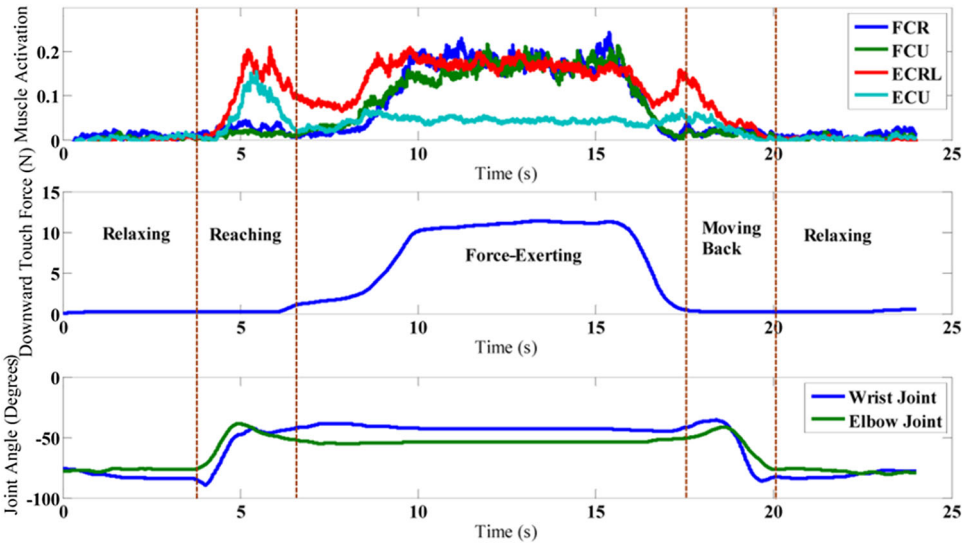

Fig. 3 Recorded data. *Upper plot* shows normalized muscle activation levels from four muscles. *Middle plot* shows recorded downward touch force from force sensor. *Lower plot* shows wrist joint and elbow joint angles recorded from MTx sensors. Different motions are labeled in middle plot

where F_i is the original prediction result and F'_i is the smoothing result. Δ is the difference between the discontinuous point and the previous point. t is the time interval for smoothing processing (set at 200 ms for this study). The minus sign (plus sign) indicates the beginning (end) of measurements.

2.5 Development of Prediction Function

Previous research has addressed the linear relationship between the musculotendon force (F_T) and the muscle activation level [$a(t)$], as defined in Eq. (4), where C_T denotes the constant coefficient [30]:

$$F_T = c_T a(t) \tag{4}$$

The proposed prediction function was derived from the dynamic equation developed from a musculoskeletal model of the downward touch motion (shown in Fig. 4a). This paper is only concerned with palm flexion and extension, and the co-activation of flexors and extensors around the forearm was counted in order to balance the torque exerted by the contact force. Thus, the dynamic equation can be written as:

$$\tau_{Flexors} - \tau_{Extensors} + \tau_{mg} = \tau_F \tag{5}$$

where τ_{Flexors} denotes the torque exerted by the flexors (FCR and FCU) while $\tau_{\text{Extensors}}$ denotes the torque exerted by the extensors (ECRL and ECU). τ_F is the torque derived from the contact force. τ_{mg} is the torque exerted by the hand's gravity force. The friction in the joint is ignored here. The gesture in which the upper arm, forearm, and hand form a line and the contact force passes through the wrist joint is referred to as the "singular gesture." During the singular gesture, the main function of the forearm's flexors and extensors is to maintain stiffness at the wrist joint, and contact force is balanced by contractions in other muscle groups. Subjects were required to avoid (to the best of their ability) the singular gesture when performing downward touch motions; such avoidance was guaranteed while recording the subjects' reference gestures.

Because the force-exerting motion is isometric, the moment arms involved in Eq. (5) can be considered constant. Substituting Eq. (4) back into Eq. (5) yields:

$$c_F F = \sum_{i=1}^{n} c_a a_i(t) + \tau_{mg} \tag{6}$$

where c_a equals the product of moment arm and constant coefficient c_T and n (=4) represents the number of muscles. c_F is the moment arm of contact torque τ_F, which was also considered constant. Dividing c_F on both sides of Eq. (6) yields:

$$F = \sum_{i=1}^{n} \omega_i a_i(t) + \tau_{mg}/c_F \tag{7}$$

where ω equals c_a/c_F. Equation (7) was used to predict the contact force after the ANN classifier recognized the force-exerting motion. To compare the effects of not considering the co-activation, $\tau_{\text{Extensors}}$ was eliminated from Eq. (5), which meant that $n = 2$ for Eq. (7).

2.6 Parameter Calibration

The parameters ω of Eq. (7) were calibrated with the BLR algorithm using data recorded from offline experiments.

Assuming that the noise in the prediction function is in Gaussian form, Eq. (7) can be written as:

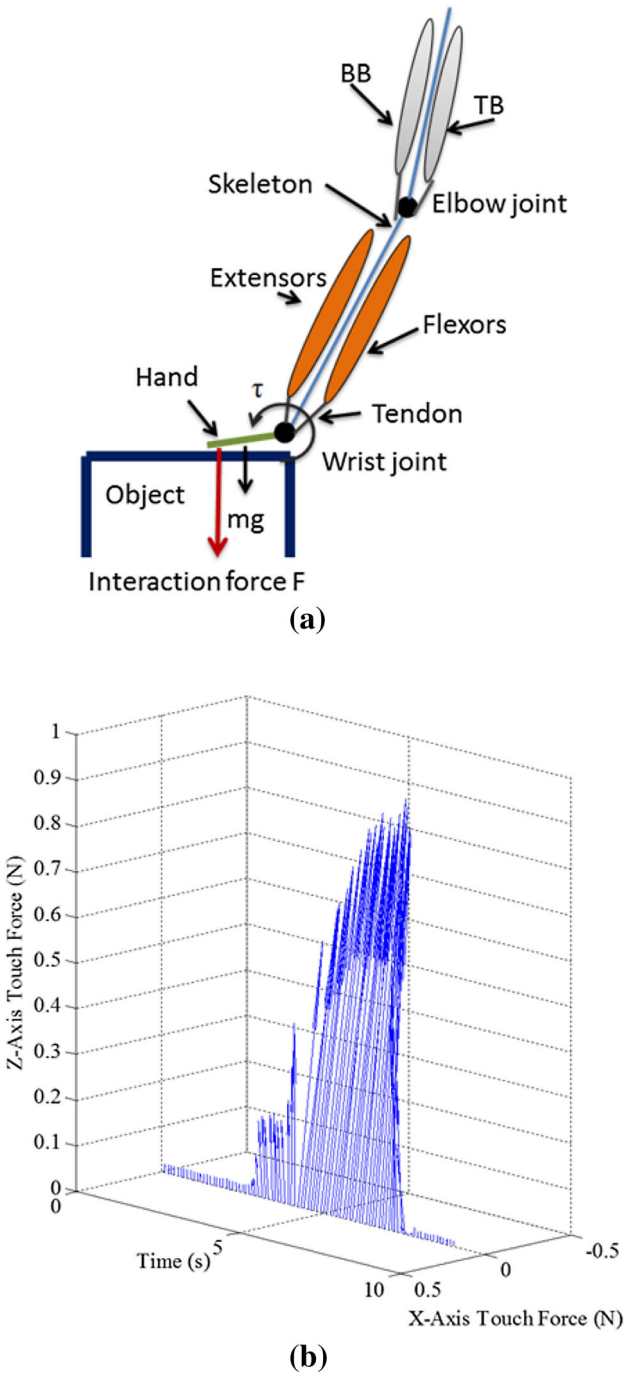

Fig. 4 **a** Proposed musculoskeletal model and **b** corresponding downward touch force. Flexors (FCR and FCU) and extensors (ECRL and ECU) of forearm were considered in musculoskeletal model. Actual force was three-dimensional. Because Z-axis had most force, X- and Y-axes are ignored for simplicity in this paper

$$F = y(\boldsymbol{a}, \boldsymbol{\omega}) + \varepsilon \tag{8}$$

where ε is a zero-mean Gaussian random variable with precision β and the bold forms of a and ω represent the vector. The following likelihood function can thus be obtained:

$$p(F|\boldsymbol{a}, \boldsymbol{\omega}, \beta) = \prod_{n=1}^{M} N(F_n|\boldsymbol{\omega}^T a_n, \beta^{-1}) \tag{9}$$

where M denotes the number of samples used for calculation.

It was assumed that the prior probability distribution over $\boldsymbol{\omega}$ was also in the form of a Gaussian distribution:

$$p(\boldsymbol{\omega}) = N(\boldsymbol{\omega}|\boldsymbol{m}_0, \boldsymbol{S}_0) \tag{10}$$

where $\boldsymbol{m}_0$ denotes the mean value of $\boldsymbol{\omega}$ and $\boldsymbol{S}_0$ denotes the covariance.

Because the posterior distribution is proportional to the product of the likelihood function and the prior, the following function is obtained:

$$p(\boldsymbol{\omega}|F) = N(\boldsymbol{\omega}|\boldsymbol{m}_N, \boldsymbol{S}_N) \tag{11}$$

where

$$\boldsymbol{m}_N = \boldsymbol{S}_N \cdot (\boldsymbol{S}_0^{-1}\boldsymbol{m}_0 + \beta\Phi^T F) \tag{12}$$

$$\boldsymbol{S}_N^{-1} = \boldsymbol{S}_0^{-1} + \beta\Phi^T\Phi \tag{13}$$

$\boldsymbol{m}_N$ denotes the mean of $\boldsymbol{\omega}$ given the condition of F, and $\boldsymbol{S}_N$ is the covariance. The evidence approximation method was adopted to calculate $\boldsymbol{m}_N$ and $\boldsymbol{S}_N$. As there were 5 × 5 sets of data, a "cross-validation" selection criterion was adopted to obtain local optimal parameters. In this criterion, one set of the experimental data was used to calculate the parameters; the performance of those parameters was assessed by evaluating the RMS errors with the remaining data. This procedure was performed on all experimental data and those with the smallest RMS errors were selected as the final optimal parameters.

3 Results

3.1 Performance of ANN Classifier

Experimental results of the ANN classifier's recognition accuracy rates are listed in Table 1. The average accuracy rate for the seven subjects is 96.8 %. The average time consumption for motion recognition with the ANN

Table 1 Recognition accuracy rates for seven subjects

	Subject						
	A	B	C	D	E	F	G
Recognition accuracy rate (%)	96.0	97.4	94.7	96.7	97.4	98.2	97.1

classifier was 0.0034 ms, calculated with a personal computer (Inter Core2 Duo E7500 CPU at 2.93 GHz, 4 GB of RAM, Windows 7). A detailed classification confusion matrix of one classifier is plotted in Fig. 5a, where numbers 1 through 4 represent the relaxed, reaching, force-exerting, and returning motions, respectively. The recognition accuracy rate for the classifier shown in that figure is 96.0 %. In particular, the recognition accuracy rate for the force-exerting motion is quite high (99.0 % in this case), which indicates that using ANN as the classifier is suitable in our case. One set of online experimental results for motion classification is plotted in Fig. 5b, where the upper plot shows the recognized motions (depicted as lines with different colors) while the corresponding contact force and joint angles are plotted in the middle and lower plots, respectively.

3.2 Contact Force Prediction

The entire time consumption of a single-loop contact force prediction was within 0.3 ms, including data collection, pre-processing, motion recognition, and prediction. Table 2 lists the experimental results of RMS errors and linear CCs of contact force predictions for the downward touch motion with various high-pass cutoff frequencies. A set of online prediction results with a high-pass cutoff

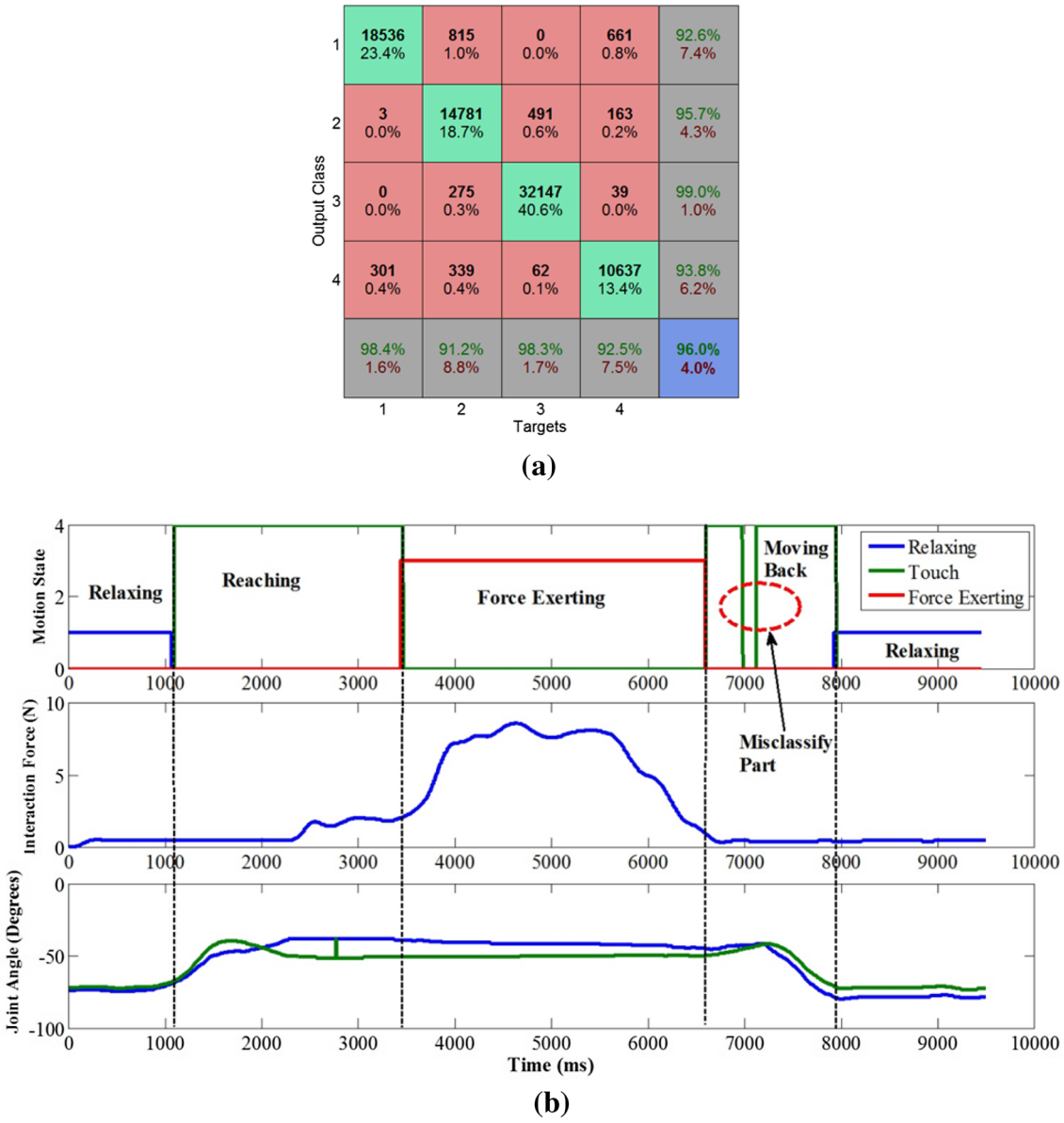

Fig. 5 **a** Classification confusion matrix of one classifier. Recognition accuracy rate for motion 3 was most important one for this study. **b** *Upper plot* shows classification results. Misclassification did not affect prediction results because only force-exerting motion was affected. *Middle and bottom plots* show the corresponding contact force and joint angles, respectively

Table 2 RMS errors (N) and CCs of downward touch force predictions

High-pass cut-off frequency (Hz)						
Subject	RMS errors			Linear CCs		
	20	200	400	20	200	400
A	1.40 ± 0.80	1.33 ± 0.78	1.42 ± 0.62	0.88	0.91	0.92
B	2.27 ± 1.40	2.20 ± 1.42	2.25 ± 1.38	0.79	0.86	0.86
C	1.69 ± 1.04	1.72 ± 1.03	1.65 ± 0.95	0.87	0.91	0.92
D	1.62 ± 0.81	1.91 ± 0.79	1.50 ± 0.81	0.85	0.92	0.93
E	1.64 ± 0.79	1.38 ± 0.64	1.60 ± 0.87	0.87	0.91	0.91
F	1.71 ± 0.89	1.69 ± 0.66	1.70 ± 0.79	0.89	0.90	0.91
G	1.81 ± 1.12	1.73 ± 0.89	1.51 ± 1.00	0.88	0.91	0.91

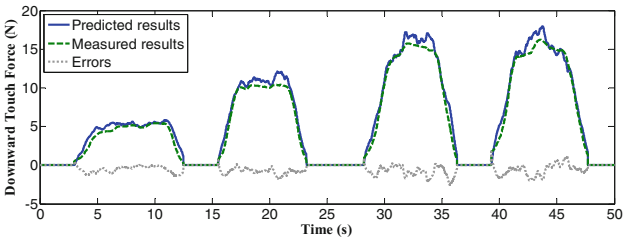

Fig. 6 On-line prediction results. Solid blue line is predicted results. Measured results are plotted with *green dashed line*. Errors between the two are plotted with *dotted gray line*

frequency of 200 Hz is shown in Fig. 6. The experimental results show that (except for subject B) the RMS errors of all subjects were below 2.0 N (subject B's RMS error was 2.27 N). Although the RMS errors and linear CCs of the different cutoff frequencies were slightly different, the high-pass cutoff frequency had no significant effect on them ($p > 0.5$). The experimental results of the effect of flexor and extensor co-activation on RMS errors and CCs are plotted in Fig. 7. The results were obtained using a high-pass cutoff frequency of 200 Hz. The effect of co-activation for RMS errors and CCs is significant ($p < 0.001$). The average RMS error is 1.70 ± 0.30 N with co-activation and 4.90 ± 1.08 N without it. Linear CCs are 0.90 with co-activation and 0.59 without.

The effect of the smoothing algorithm is shown in Fig. 8, where the upper and lower plot shows the prediction results without and with smoothing, respectively.

By using the proposed smoothing algorithm, a therapist can accurately grade the patient's predicted force in real time.

4 Discussion

This study aimed to build a muscle strength assessment system for home-based tele-rehabilitation. Two crucial aspects for clinical application were considered and are

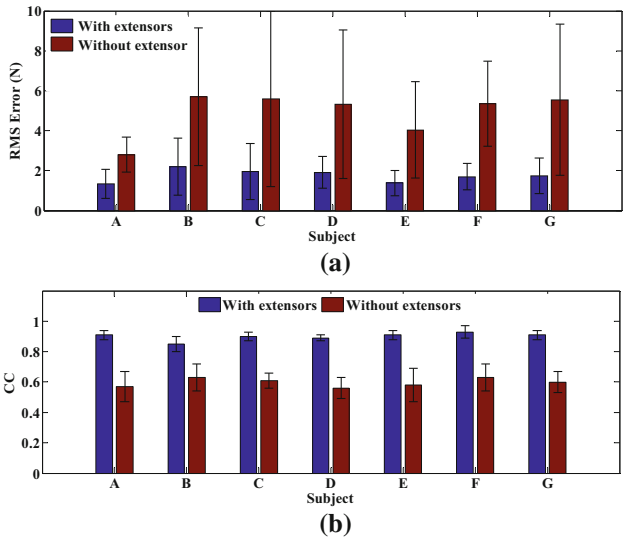

Fig. 7 Effect of co-activation for force prediction. **a** Comparison results of RMS errors. **b** Comparison results of CC. Co-activation of flexors and extensors had significant effect on RMS errors and CCs between predicted and measured results

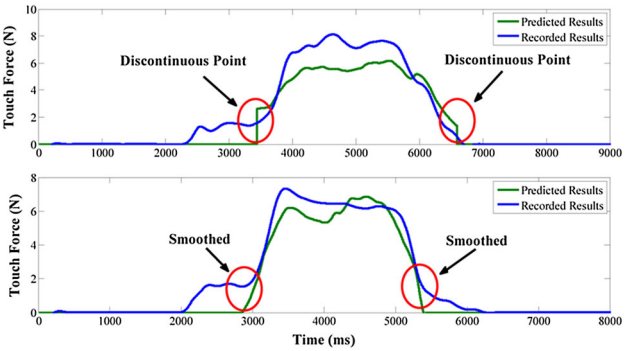

Fig. 8 Effect of smoothing algorithm. *Upper plot* shows experimental results without smoothing (two discontinuous points would cause sensation of impact in remote force evaluation experiment). *Lower plot* shows results with smoothing (note that smoothing eliminates sensation of impact)

summarized as follows. First, sEMG provides a basic method for determining the amount of force exerted. A method for predicting motion based on sEMG that is more simplistic than existing methods was proposed, which can easily be extended to general rehabilitation training with more motions. Second, traditional movement-restricting apparatuses, which increase the burden on patients (particularly for home-based training), were avoided. Instead, a more effective motion detection method with MTx sensors was proposed for use during tele-assessment situations. Instead of using complicated explicit dynamic movement modeling, an ANN classifier was adopted to identify the force-exerting motion from the group of four identified motions involved in the subjects' downward touch movement. The muscle force was assessed with isometric contraction, for which the ANN classifier is adequate, as indicated by the obtained accuracy rates. However, although accuracy rates were quite high (approximately 99 % for the force-exerting motion), the recognition resolution makes it impossible to classify the force-exerting motion at the moment that it happens. Some researchers [28] have discussed similar problems occurring during class transitions and dynamic movement phases; in those cases, the recognition results were affected. Thus, post-process correcting methods have been proposed to improve the classification accuracy rate. However, merely improving the accuracy rate does not seem to be enough to fix our problem (the accuracy rate with the proposed method is as high as 99 %); instead, the proposed proportional smoothing method must be used. Without this smoothing method, a therapist may feel a significant sensation of impact at the beginning and end of the force-exerting motion in a remote force evaluation. Furthermore, the functions involved are not complex and can be easily implemented on another hardware platform. Consequently, the proposed method is suitable for a wide range of applications.

During force prediction, the high-pass cutoff frequency has no significant effect on the RMS errors and linear CCs of the downward touch contact force prediction. In Potvin and Brown's study [31], a high-pass filter with a cutoff frequency of 400 Hz improved the EMG–force estimation of biceps brachii; furthermore, in Staudenmann et al.'s study [32], a high-pass filter benefitted the moment estimation of trunk muscles. In Potvin and Brown's case, the relationship was focused on a single muscle; in Staudenmann's case, suppression of ECG contamination was one probable factor in the demonstrated improvement. In our case, the contact force was predicted based on the model of multi-muscle movement results, rather than just one muscle, and no obvious ECG contamination was found.

Co-activation of flexors and extensors is also considered in this paper. The performance of the prediction results for RMS errors and linear CCs were significantly better when including the extensor in the prediction function ($p < 0.001$). These results correspond to Brown and McGill's results [33]; however, this paper studies the muscles around the forearm, while Brown and McGill studied trunk muscles. Consequently, it is strongly recommended to take into account the effect of co-activation when predicting the downward touch force of forearm muscles.

The joint angle was another factor affecting the EMG–force relationship [21]. Different joint angles result in varying muscle length, muscle-moment arm, and the relative location of the innervation zone with respect to the electrode used to record sEMG signals. Therefore, a movement-restricting apparatus is often used to constrain the joint angle. Because the proposed method aims to be applied to home-based muscle strength assessments, it is inconvenient for patients to wear such devices when performing the assessment. However, the utilized MTx sensors provided "soft restrictions" on the subject's motion. During the online experiment, this soft restriction was less rigid; therefore, subjects were able to skip the step of adjusting their gesture to match the reference gesture, and thus were able to directly perform the subject task at hand. Note that subjects may have remembered the general position from the offline experiment and that the range of joint angles was within a limited range. The average range of the wrist joint angle was $3.00° \pm 2.47°$, and that of the elbow joint was $2.90° \pm 1.18°$. These ranges are within the increments usually studied in the literature. However, the proposed protocol is more practical, and the experimental results verify that the proposed method can guarantee the validity of force predictions without the use of any restricting apparatus.

5 Conclusion

In this study, a novel contact force prediction method for downward touch motion, using only sEMG signals, was proposed. The proposed method can provide acceptable, accurate prediction results with RMS errors of below 2.3 N. The sEMG signal is of great importance in the understanding of muscle activities. A remote force evaluation experiment validated the real-time performance of the proposed method and provides an example of its application; it can transmit the sensation of touch to a therapist at a remote location. Furthermore, the effects of high-pass cutoff frequency and of the co-activation of flexors and extensors on EMG–force predictions were also discussed. The high-pass cutoff frequency has no significant effect on RMS errors and linear CCs, but it is strongly recommended that the co-activation of the forearm's flexors and extensors

be considered when predicting the contact force of downward touch motions.

This study primarily focused on the wrist joint for downward touch motion. Because the proposed method predicts contact force as an output of the function of muscle groups instead of studying individual muscles, the method can be easily used for predicting other motions (e.g., a push motion). Future study endeavors will extend the proposed predicting method to other motions with more elegant musculoskeletal models to provide a comprehensive assessment of the patient. Moreover, the designed exoskeleton device can train not only the wrist joint but also the elbow joint with multiple degrees of freedom.

Acknowledgments This research was partly supported by National Natural Science Foundation of China (61375094), Key Research Program of the National Science Foundation of Tianjin (13JCZDJC26200), National High-Tech Research and Development Program of China (2015AA043202), and the Japan Society for the Promotion of Science (JSPS) Grants-in-Aid for Scientific Research (KAKENHI) (15K2120).

References

1. Lloyd-Jones, D., Adams, R. J., Brown, T. M., Carnethon, M., Dai, S., De Simone, G., et al. (2010). Heart disease and stroke statistics–2010 update: A report from the American Heart Associate. *Circulation, 121*, 46–215.
2. Song, Z., Guo, S., & Fu, Y. (2011). Development of an upper extremity motor function rehabilitation system and an assessment system. *International Journal of Mechatronics Automation, 1*, 19–28.
3. Song, Z., Guo, S., Pang, M., Zhang, S., Xiao, N., Gao, B., & Shi, L. (2014). Implementation of resistance training using an upper-limb exoskeleton rehabilitation device for elbow joint. *Journal of Medical and Biological Engineering, 34*, 188–196.
4. Zhang, S., Guo, S., Gao, B., Hirata, H., & Ishihara, H. (2015). Design of a novel telerehabilitation system with a force-sensing mechanism. *Sensors, 15*, 11511–11527.
5. Park, H. S., Peng, Q., & Zhang, L. Q. (2008). A portable telerehabilitation system for remote evaluations of impaired elbows in neurological disorder. *IEEE Transactions on Neural Systems and Rehabilitation Engineering, 16*, 245–254.
6. Disselhorst-Klug, C., Schmitz-Rode, T., & Rau, G. (2009). Surface electromyography and muscle force: Limits in sEMG-force relationship and new approaches for applications. *Clinical Biomechanics, 24*, 225–235.
7. Staudenmann, D., Roeleveld, K., Stegeman, D. F., & van Dieën, J. H. (2010). Methodological aspects of SEMG recordings for force estimation—a tutorial and review. *Journal of Electromyography and Kinesiology, 20*, 375–387.
8. Savelberg, H. H., & Herzog, W. (1997). Prediction of dynamic tendon forces from electromyographic signals: An artificial neural network approach. *Journal of Neuroscience Methods, 78*, 65–74.
9. Cavallaro, E., Rosen, J., Perry, J. C., Burns, S., & Hannaford, B. (2005). Hill-based model as a myoprocessor for a neural controlled powered exoskeleton arm-parameters optimization. *Proeedings of the IEEE International Conference on Robotics & Automation*, 4525–4530.
10. Cavallaro, E. E., Rosen, J., Perry, J. C., & Burns, S. (2006). Real-time myoprocessors for a neural controlled powered exoskeleton arm. *IEEE Transactions on Biomedical Engineering, 53*, 2387–2396.
11. Manal, K., & Buchanan, T. S. (2003). A one-parameter neural activation to muscle activation model: Estimating isometric joint moments from electromyograms. *Journal of Biomechanics, 36*, 1197–1202.
12. Potvin, J. R., Norman, R. W., & McGill, S. M. (1996). Mechanically corrected EMG for the continuous estimation of erector spine muscle loading during repetitive lifting. *European Journal of Applied Physiology and Occupational Physiology, 74*, 119–132.
13. Lloyd, D. G., & Besier, T. F. (2003). An EMG-driven musculoskeletal model to estimate muscle forces and knee joint moments in vivo. *Journal of Biomechanics, 36*, 765–776.
14. Fleischer, C., & Hommel, G. (2008). A human–exoskeleton interface utilizing electromyography. *IEEE Transactions on Robotics, 24*, 872–882.
15. Fleischer, C., Reinicke, C., & Hommel, G. (2005). Predicting the intended motion with EMG signals for an exoskeleton orthosis controller. *Proceedings of IEEE International Conference on Intelligent Robot and Systems*, 2029–2034.
16. Staudenmann, D., Kingma, I., Stegeman, D. F., & van Dieën, J. H. (2005). Towards optimal multi-channel EMG electrode configurations in muscle force estimation: A high density EMG study. *Journal of Electromyography Kinesiology, 15*, 1–11.
17. Artemiadis, P. K., & Kyriakopoulos, K. J. (2011). A switching regime model for the EMG-based control of a robot arm. *IEEE Transactions on Systems Man Cybernatics B, 41*, 53–63.
18. Amarantini, D., & Martin, L. (2004). A method to combine numerical optimization and EMG data for the estimation of joint moments under dynamic conditions. *Journal of Biomechanics, 37*, 1393–1404.
19. SENIAM project. http://www.seniam.org/.
20. Lew, H. L., & Tsai, S. J. (2007). *Johnson's practical electromyography* (4th ed.). Philadelphia: Lippincott Williams & Wilkins.
21. Hashemi, J., Morin, E., Mousavi, P., Mountjoy, K., & Hashtrudi-Zaad, K. (2012). EMG-force modeling using parallel cascade identification. *Jounal of Electromyography Kinesiology, 22*, 467–477.
22. Thelen, D. G., Schultz, A. B., Fassois, S. D., & Ashton-Miller, J. A. (1994). Identification of dynamic myoelectric signal-to-force models during isometric lumbar muscle contractions. *Journal of Biomechanics, 27*, 907–919.
23. Buchanan, T. S., Lloyd, D. G., Manal, K., & Besier, T. F. (2004). Neuromusculoskeletal modeling: Estimation of muscle forces and joint moments and movements from measurements of neural command. *Journal of Applied Biomechanics, 20*, 367–395.
24. Manal, K., Gonzalez, R. V., Lloyd, D. G., & Buchanan, T. S. (2002). A real-time EMG driven virtual arm. *Computers in Biology and Medicine, 32*, 25–36.
25. Tang, X., Liu, Y., Lv, C., & Sun, D. (2012). Hand motion classification using a multi-channel surface electromyography sensor. *Sensors, 12*, 1130–1147.
26. Ju, Z., Ouyang, G., Wilamowska-Korsak, M., & Liu, H. (2013). Surface EMG based hand manipulation identification via nonlinear feature extraction and classification. *IEEE Sensors Journal, 13*, 3302–3311.
27. Chen, X., & Wang, Z. J. (2013). Pattern recognition of number gestures based on a wireless surface EMG system. *Biomedical Signal Process Control, 8*, 184–192.
28. Amsüss, S., Goebel, P. M., Jiang, N., Graimann, B., Paredes, L., & Farina, D. (2014). Self-correcting pattern recognition system of

surface EMG signals for upper limb prosthesis control. *IEEE Transactions on Biomedical Engineering, 61*, 1167–1176.
29. Bu, N., Okamoto, M., & Tsuji, T. (2009). A hybrid motion classification approach for EMG-based human–robot interfaces using Bayesian and neural networks. *IEEE Transactions on Robotics, 25*, 502–511.
30. Pang, M., Guo, S., Huang, Q., Ishihara, H., & Hirata, H. (2015). Electromyography-based quantitative representation method for upper-limb elbow joint angle in sagittal plane. *Journal of Medical and Biological Engineering, 35*, 165–177.
31. Potvin, J. R., & Brown, S. H. M. (2004). Less is more: High pass filtering, to remove up to 99 % of the surface EMG signal power, improves EMG-based biceps brachii muscle force estimates. *Journal of Electromyography Kinesiology, 14*, 389–399.
32. Staudenmann, D., Potvin, J. R., Kingma, I., Stegeman, D. F., & van Dieën, J. H. (2007). Effects of EMG processing on biomechanical models of muscle joint systems: Sensitivity of trunk muscle moments, spinal forces, and stability. *Journal of Biomechanics, 40*, 900–909.
33. Brown, S. H., Brookham, R. L., & Dickerson, C. R. (2010). High-pass filtering surface EMG in an attempt to better represent the signals detected at the intramuscular level. *Muscle and Nerve, 41*, 234–239.